ORIGINAL PAPER

Theoretical studies on the kinetics and mechanism of the gas-phase reactions of CHF_2OCHF_2 with OH radicals

Asit K. Chandra

Abstract The mechanism, kinetics and thermochemistry of the gas-phase reactions between CHF_2OCHF_2 (HFE-134) and OH radical are investigated using the high level ab initio G2(MP2) and hybrid density functional model MPWB1K quantum chemical methods. Two relatively close in energy conformers are found for CHF_2OCHF_2 molecule; both of them are likely to be important in the temperature range (250-1000 K) of our study. The hydrogen abstraction pathway for both the conformers with OH radical is studied and the rate constants are determined for the first time in a wide temperature range of 250 – 1000 K. The G2(MP2) calculated total rate constant value of 2.9×10^{-15} cm^3 molecule^{-1} s^{-1} at 298 K is found to be in very good agreement with the reported experimental value of 2.4×10^{-15} cm^3 molecule^{-1} s^{-1} at 298 K. The heats of reaction for CHF_2OCHF_2+OH reaction is computed to be -13.2 kcal mol^{-1}. The atmospheric lifetime of CHF_2OCHF_2 is expected to be around 12 years.

Keywords Hydrogen abstraction · CHF_2OCHF_2 · OH radical · G2(MP2) · Rate constants

Introduction

The adverse environmental impact of chlorofluorocarbons (CFCs) [1] in stratospheric ozone depletion and global warming has led to international agreements to replace these

A. K. Chandra (✉)
Department of Chemistry, North-Eastern Hill University,
Shillong 793 022, India
e-mail: akchandra@nehu.ac.in

compounds with more environmentally acceptable compounds. The commercial production of CFCs is therefore being phased out according to the Montreal Protocol and its subsequent amendments and adjustments [2]. Hydrofluoroethers (HFE's) have long been proposed as a new generation of alternatives for chlorofluorocarbons (CFC) and hydrochlorofluorocarbons (HCFC) in applications such as refrigerants, cleaning solvents, foam-blowing agents, aerosol propellants and fire-extinguishing agent etc. [3–7], since they do not contain chlorine or bromine atoms and they do not contribute to stratospheric ozone loss through the well-established chlorine-based catalytic cycles [8]. Also HFEs are probably more reactive in the troposphere due to the presence of –O- ether linkage [9]. Although HFEs do not contain Cl atom and have zero ozone depletion potential, they are potential greenhouse gases because of their strong absorption in the range of 1000–3000 cm^{-1} [10, 11]. Reactions of HFEs with OH radicals constitute the main degradation channel of HFEs in the troposphere [12]. Therefore, it is important to study the reactivity of HFEs against OH radicals for the evaluation of the atmospheric lifetime of HFEs. Thus, there are many recent experimental and theoretical studies on the reactions of HFEs with OH radical [13–22].

In this present work, we have studied in detail the hydrogen abstraction reactions between CHF_2OCHF_2 and OH radical (R1) by using quantum chemical methods.

$$CHF_2OCHF_2 + OH \rightarrow CHF_2OCF_2 + H_2O \qquad (R1)$$

This reaction was first studied by Zhang et al. in 1992 using a flash photolysis resonance fluorescence (FPRF) technique and reported a rate constant of 2.53×10^{-14} cm^3 molecule^{-1} s^{-1} at 296 K [23]. Subsequently the reaction was studied experimentally by several other authors using pump and probe laser-

induced fluorescence [24], flash photolysis resonance fluorescence (FPRF) technique [25] and the relative rate method [26] within a temperature range from 277 K to 393 K. Their reported rate constant values vary within a range of 2.3×10^{-15} to 2.9×10^{-15} cm^3 molecule^{-1} s^{-1}, which is almost an order of magnitude smaller than the value reported by Zhang et al. [23]. Later, Wilson et al. [27] performed another experimental study by using a relative method and they also reported a rate constant value of 2.23×10^{-15} cm^3 molecule^{-1} s^{-1} at 298 K. Experimentally the kinetics of reaction (R1) are now well established with $k_{OH} = 2.4 \times 10^{-15}$ cm^3 molecule^{-1} s^{-1} at 298 K, and the atmospheric lifetime of CHF_2OCHF_2 has been estimated to be 15 years [28].

However, experimental study provides mainly the total rate constant and it is difficult to get the mechanism and detailed picture of a reaction, especially for multichannel reactions. Theoretical investigations, on the other hand, can provide the mechanism and thermochemistry of this reaction, and give information about the relative importance of each channel. To the best of our knowledge, the only theoretical calculation on reaction (R1) was performed by Francisco et al. in 1999 using DFT based B3LYP method [29]. However, the barrier height obtained from their calculation (0.8 kcal mol^{-1}) was far below the measured activation barrier of 4.0 kcal mol^{-1} by Hsu and DeMore using a relative rate technique [26] and no rate constant calculation was performed. Moreover, our recent study on the reaction between CHF_2OCHF_2 and Cl atom has revealed that CHF_2OCHF_2 has two possible low energy conformers and both of them need to be considered for any kinetic study [30]. Hence we set out to study the reaction (R1) using ab initio G2(MP2) and DFT based MPWB1K quantum chemical methods and kinetic modeling for better understanding of this reaction.

We present here the potential energy profile (including geometries, energies and vibrational frequencies of reactants, transition states, products) and kinetic data for this reaction along with the relative importance for each reaction channel. We also report here for the first time the rate constant for the reaction in a wide temperature range of 250 – 1000 K.

Computational method

The structures of reactants (CHF_2OCHF_2 and OH), transition states (TS) for hydrogen abstraction reactions, radicals (CHF_2OCF_2) produced after hydrogen abstraction from CHF_2OCHF_2 were optimized using the MPWB1K/6-31+G(d,p) method [31]. The MPWB1K method is specifically designed for kinetic and thermochemical modeling and is known to produce reliable results [30–34].

Vibrational frequency calculations were performed at each stationary point to characterize the minimum energy equilibrium structure (having all real frequencies) and transition state (with one imaginary frequency). Normal mode analysis of the TS also confirms that the imaginary frequency in TS correspond to the coupling of stretching modes of the breaking C-H and forming O-H bonds. Finally high level ab initio G2(MP2) [35] calculations were performed for all the stationary points along the potential energy surface of the reaction at the MPWB1K optimized structure for further refinement of our results. The unrestricted open-shell formalism was used for the calculation of radicals and transition states. The spin contamination for open-shell systems was found to be low, with < S2 > value never exceeding 0.7611 at the DFT level and 0.7857 at the HF level. The zero point energy (ZPE) obtained at the MPWB1K level was used when estimating the G2(MP2) energy [35]. This dual level calculations (G2(MP2)//MPWB1K) is known to produce reliable kinetic data [30, 34, 36]. All electronic structure calculations were performed by using the Gaussion-03 suite of program [37].

The rate constant for hydrogen abstraction reaction was estimated using the conventional transition state theory (TST) equation [38]:

$$k(T) = \sigma_r \Gamma(T) \frac{k_B T}{h} \frac{q_{TS}(T)}{q_{HFE}(T) . q_{OH}(T)} e^{-\Delta E_0^{\#}/RT}, \quad (1)$$

where $q_x(T)$ represents the partition function for the species x (TS, HFE and OH) at temperature T, k_B is the Boltzmann constant, $\Delta E_0^{\#}$ is the barrier height and σ_r is the degeneracy of each reaction channel. The $\Gamma(T)$ is the correction factor for tunneling in H-abstraction reaction. Tunneling is an important quantum mechanical phenomenon and plays an important role for H-atom transfer reactions. The tunneling correction to the rate constant was estimated by using the Eckart's unsymmetric barrier method [39]. In this method, the reaction path through TS is fitted first in a model potential function

$$V(y) = -\frac{Ay}{1-y} - \frac{By}{(1-y)^2}, \quad (2)$$

where $y = -\exp(2\pi x/L)$ and x is the displacement along the reaction coordinate and L is a characteristic length [39]. The A and B are two parameters that depend upon forward and reverse barrier heights. The $\Gamma(T)$ was then estimated by numerically integrating the tunneling factor, $\alpha(E)$, for this potential function over all possible values of energy and divided by the classical probability [40],

$$\Gamma(T) = e^{\Delta E^{\#}/k_b T} \int_{0}^{\infty} e^{-E/k_b T} \alpha(E) d(E/k_b T). \quad (3)$$

The value of $\Gamma(T)$ vary in the range of 65.8 at 250 K to almost 1 at 1000 K for different reaction channels of this reaction.

Partition functions were calculated using the rigid rotor and harmonic oscillator (HO) model and barrier height was estimated from the energy difference including ZPE between TS and reactants. The electronic partition function for OH radical was calculated considering the splitting of 139.7 cm^{-1} of the $^2\pi$ ground state [41]. The low frequency torsional motion of O-CHF$_2$ moiety was treated as HO only since hindered rotor correction for such motion in molecule and TS would likely to cancel each other in the TST expression and the rotation of OH in TS was suppressed by hydrogen bonding. Moreover, the q^{HIN}/q^{HO} correction estimated by Truhlar's procedure [42] was seen to be only 1.02 for the most dominant reaction channel.

The reaction is seen to proceed through the formation of pre- and post-reaction complexes (discussed in the next section). In order to take into account the effect of pre- and post-reactive complex on reaction kinetics, we have followed the proposal made by Singleton and Cvetanovic [43] and elsewhere [36]. As discussed, the reaction follows a general path where two reactants (HFE and OH) first form a complex (HFE..OH):

$$HFE + OH \leftrightarrow HFE..OH \rightarrow Products$$

If k_f and k_r are the rate constants for the forward and reverse reactions of the first step (complex formation), respectively, and k_1 is the rate constant for the second step, then a steady state analysis gives the total rate constant (k) for the overall reaction as,

$$k = \frac{k_f k_1}{k_r + k_1}. \tag{4}$$

Following the argument of Singleton and Cvetanovic [43] and others [44], one can expect k_r to be considerably greater than k_1 and this leads to,

$$k = \frac{k_f k_1}{k_r} = \left(\frac{A_f A_1}{A_r}\right) e^{-(\Delta E_f + \Delta E_1 - \Delta E_r)/RT}$$

$$= \Gamma \frac{k_B T}{h} \frac{Q_{TS}}{Q_R} e^{-(E_{TS} - E_R)/RT}, \tag{5}$$

where A's are the pre-exponential factors, ΔE_f and ΔE_r are the barrier heights for the forward and reverse reaction of the first step (complex formation) and ΔE_1 is the barrier height for the second step. Thus apparently the final expression (Eq. 5) for estimating rate constant and barrier height turns out to be the usual TST expression (Eq. 1) for the estimation of rate constant and barrier height of a direct reaction, irrespective of the energy of pre-reactive complex. Of course, the formation of pre- and post-reaction complex modifies the shape of potential energy surface for the reaction and hence affects the tunneling factor (Γ) and as a result the rate constant for hydrogen abstraction also changes. Therefore Eq. 1 was used for the rate constant calculation

taking into account the effect of pre- and post-reaction complexes on tunneling factor.

Results and discussion

Structure and energetics

Geometry optimization of CHF$_2$OCHF$_2$ molecule predicts two possible conformers (SC1 and SC2) and their structures are shown in Fig. 1. Among these two conformers of CHF$_2$OCHF$_2$, SC1 is the more stable conformer and SC2 is seen to be relatively close in energy (~1 kcal mol^{-1}). The two H-atoms in SC1 conformer are stereographically non-equivalent, whereas SC2 has a C$_2$ symmetry and both the H-atoms are equivalent. Since these two conformers of CHF$_2$OCHF$_2$ are closer in energy, both of them (SC1 and SC2) need to be considered while studying reaction (R1). On the other hand, two conformers for the CHF$_2$OCF$_2$ radical are observed from our calculations. Both of them are of almost equal energy and therefore should exist in equal population in an equilibrium mixture.

A schematic diagram of the reaction energy profile of the reaction between CHF$_2$OCHF$_2$+OH is shown in Fig. 2. We could locate one transition state (TS) each for hydrogen abstraction by OH radical from the C2-H4 (TS1$_{SC1}$) and C3-H7 (TS2$_{SC1}$) bond of the SC1 conformer of CHF$_2$OCHF$_2$. These two reaction channels originating from the SC1 conformer of CHF$_2$OCHF$_2$ are henceforth designated as RP1$_{SC1}$ and RP2$_{SC1}$, respectively. Meanwhile, only one TS (TS$_{SC2}$) was found for hydrogen abstraction from the SC2 conformer of CHF$_2$OCHF$_2$, since both the H-atoms are equivalent and this channel is marked as RP3$_{SC2}$. The MPWB1K optimized structures for all the TS and product radicals are also given in Fig. 1 along with some key geometrical parameters, whereas the detailed structures are given in Table 1. The breaking C-H bond and the forming O...H bond in TS structures are found to be 14 % and 30 % longer than the C-H bond length in isolated CHF$_2$OCHF$_2$ and in H$_2$O molecule, respectively. It indicates the formation of an early TS which is consistent with the exothermic nature of this reaction and with the Hammond's postulate [45] that predicts reactant-like TS for exothermic reaction.

As shown in the reaction energy profile diagram (Fig. 2), the reaction takes place through the formation of pre-reactive (CR) and post-reactive (CP) complexes. The optimized structures of these complexes are given as Supplementary information in Table S.I.1. Three CR complexes associated with the three reaction channels were located during our calculations. These complexes are resulted from the weak interactions between the HFE and OH radical through the OH...O/F and C-H...O hydrogen-bonding. The OH...O distance is almost 2.3 Å, which is far longer than the usual hydrogen
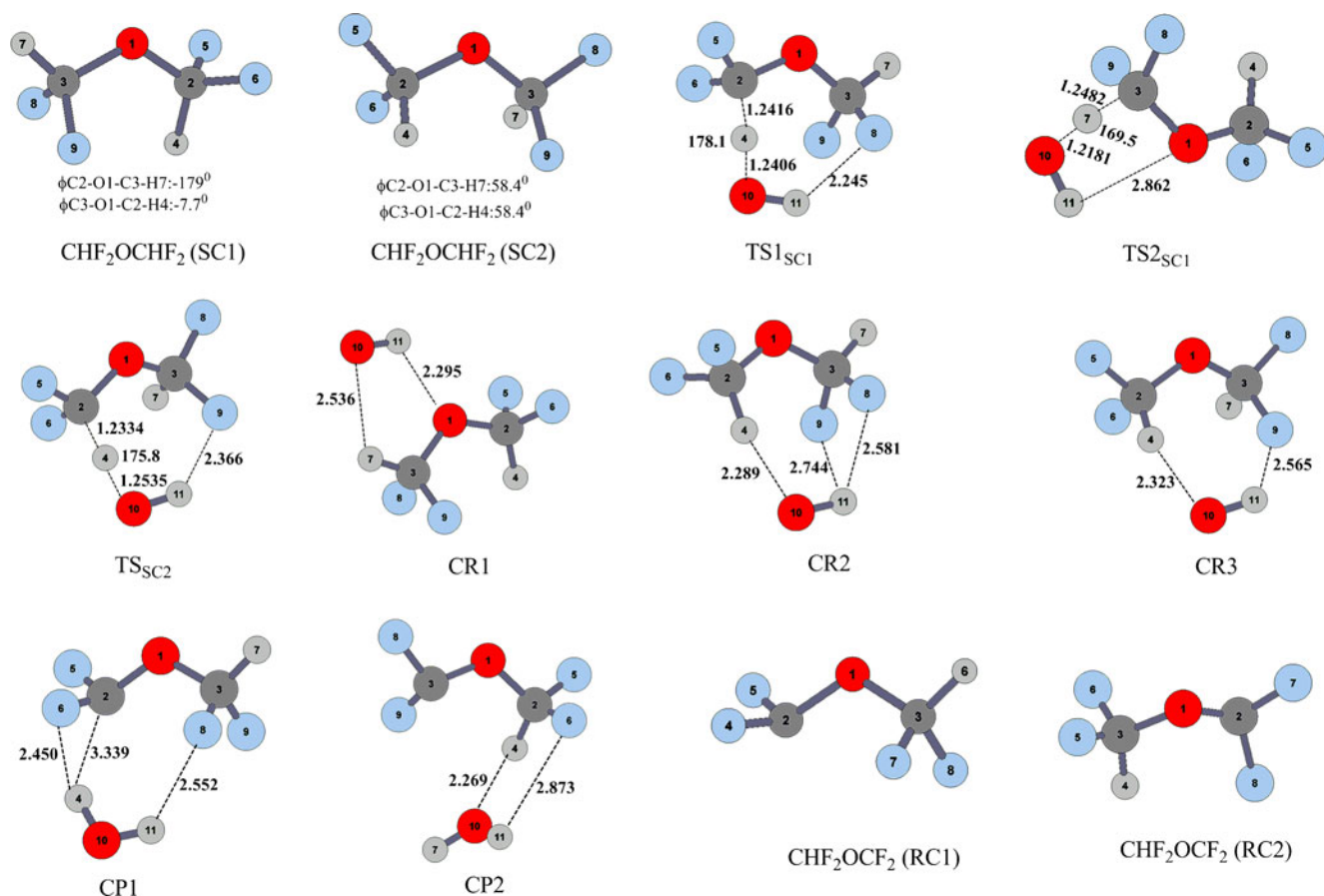
Fig. 1 MPWB1K/6-31+G(d,p) optimized structures of the two conformers of CHF_2OCHF_2 (SC1, SC2) and CHF_2OCF_2 radical (RC1, RC2), transition states for hydrogen abstraction by OH radical from two conformers of CHF_2OCHF_2 and pre- and post-reaction complexes for CHF_2OCHF_2+OH reactions. Bond lengths and angles are given in Å and degrees, respectively

bonded OH…O distance of ∼2.0 Å indicating weaker interactions than in water dimer. The post-reactive CP complexes are formed due to the weak hydrogen bonding interactions between the product radical and H_2O molecule.

The vibrational frequencies for both the conformers of CHF_2OCHF_2 molecule, CHF_2OCF_2 radical, all the transition states involved in reaction (R1), OH radical and H_2O molecule are given in Table 2 along with the rotational constants. The vibrational frequencies for the pre- and post reaction complexes are provided as Supplementary information in Table S.I.2. These data can be useful for further thermo-kinetic modeling of other reactions involving these species.

The relative energies (including ZPE) for all the species involved in reactions (R1) are given in Table 3, whereas the same is also indicated in a schematic diagram of the potential energy profile as shown in Fig. 2. The energy difference between the two conformers of CHF_2OCHF_2 is calculated to be 0.87 kcal mol^{-1} at the G2(MP2) level, respectively. This small energy difference between SC1 and SC2 implies that population of SC2 will be about 19 % at 298 K and almost 40 % at 1000 K. Hence hydrogen abstraction from both the conformers needs to be considered while estimating the total

rate constant for reaction R1. The G2(MP2) calculated barrier heights (TS1$_{SC1}$ and TS2$_{SC1}$) for hydrogen abstraction from the SC1 conformer of CHF_2OCHF_2 are 5.33 and 6.08 kcal mol^{-1}, respectively, whereas these values are 5.27 and 5.96 kcal mol^{-1} at the MPWB1K level. On the other hand, the barrier height (TS$_{SC2}$) for hydrogen abstraction from the SC2 conformer of CHF_2OCHF_2 is 4.32 and 4.04 kcal mol^{-1} at the G2(MP2) and MPWB1K level, respectively. The barrier heights obtained from the G2(MP2) results are only 0.06 to 0.28 kcal mol^{-1} higher than that obtained at the MPWB1K level. We have observed from our previous studies [33, 34, 36] and the present results that the G2(MP2) results always provide slightly better agreement with experiment than the MPWB1K results and henceforth we discuss mainly the results obtained at the G2(MP2) level.

The enthalpy of reaction ($\Delta_r H_{298}^0$) values tabulated in Table 3 for RP1$_{SC1}$ and RP3$_{SC2}$ show that both the reactions are significantly exothermic in nature at 298 K and thus thermodynamically facile. Our G2(MP2) calculated $\Delta_r H_{298}^0$ values amount to -13.01 and -13.83 kcal mol^{-1} for RP1$_{SC1}$ and RP3$_{SC2}$, respectively. Considering the relative population of the SC1 and SC2 conformers of CHF_2OCHF_2, the weighted

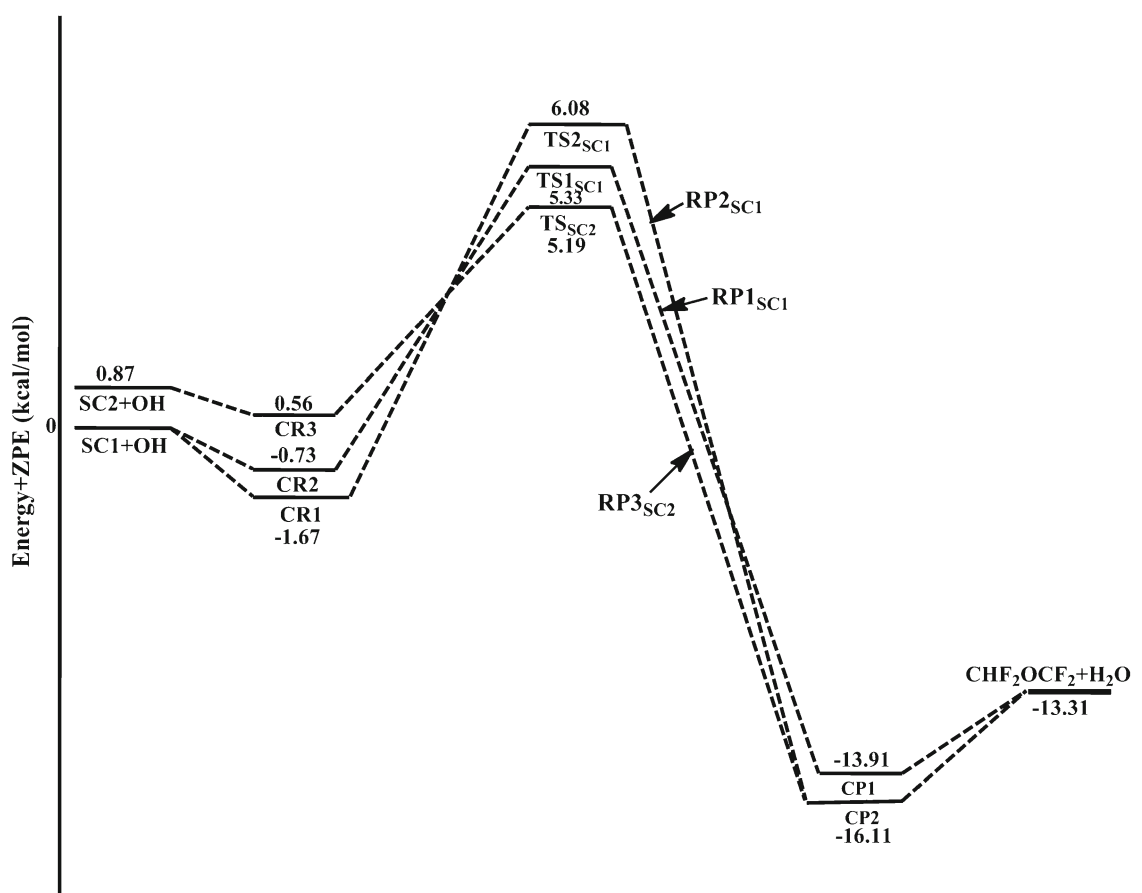**Fig. 2** Schematic diagram of the potential energy profile for the reaction between CHF_2OCHF_2 and OH radical

average of $\Delta_rH_{298}^0$ values for SC1 and SC2 conformers gives $\Delta_rH_{298}^0$ value of -13.16 kcal mol^{-1} at 298 K for the reaction (R1). The $\Delta_rH_{298}^0$ value for (R1) obtained from the reported heats of formation values for CHF_2OCHF_2 (-259.1 kcal mol^{-1})

[46], CHF_2OCF_2 (-205.1 kcal mol^{-1}) [46], OH (9.32 kcal mol^{-1}) [47], and H_2O (-57.79 kcal mol^{-1}) [47] amounts to -13.1 kcal mol^{-1}, which is quite close to our calculated value.

Table 1 MPWB1K optimized geometrical parameters of the two conformers of CHF_2OCHF_2 molecule (SC1 and SC2), transition states for hydrogen abstraction by OH radical from SC1 (TS1$_{SC1}$ and TS2$_{SC1}$) and SC2 (TS$_{SC2}$) and two conformers of CHF_2OCF_2 radical (RC1, RC2). Bond lengths and angles are given in Å and degrees, respectively. See Fig. 1 for atom numbering

Parameter	CHF_2OCHF_2 (SC1)	CHF_2OCHF_2 (SC2)	TS1$_{SC1}$	TS2$_{SC1}$	TS$_{SC2}$	CHF_2OCF_2 (RC1)	CHF_2OCF_2 (RC2)
C_2-H_4	1.0849	1.0857	1.2416	1.0854	1.2334	–	–
C_3-H_7	1.0816	1.0857	1.0817	1.2483	1.0851	1.0820	1.0855
O_1-C_2	1.3720	1.3463	1.3642	1.3800	1.3551	1.3488	1.3406
O_1-C_3	1.3531	1.3463	1.3575	1.3445	1.3685	1.3567	1.3751
C2-F5/F4	1.3337	1.3236	1.3169	1.3280	1.3127	1.3160	1.3051
C2-F6/F5	1.3316	1.3469	1.3240	1.3308	1.3343	1.3093	1.3281
C3-F8/F7	1.3428	1.3236	1.3481	1.3305	1.3214	1.3355	1.3237
C3-F9/F8	1.3442	1.3469	1.3340	1.3292	1.3462	1.3357	1.3353
H_4-O_{10}	–	–	1.2406	–	1.2535	–	–
H_7-O_{10}	–	–	–	1.2182	- -	–	–
$C_2O_1C_3$	116.6	115.8	118.7	117.0	116.8	116.9	116.1

Table 2 Harmonic vibrational frequencies (cm^{-1}) and rotational constants (GHz, within bracket) calculated at MPWB1K/6-311+G(d, p) level for CHF$_2$OCHF$_2$+OH system

System	Frequencies (cm^{-1})	$<S^2>$[a]
CHF$_2$OCHF$_2$ (SC1)	17, 81, 199, 409, 469, 541, 600, 648, 816, 1072, 1157, 1204, 1214, 1227, 1291, 1407, 1417, 1448, 1488, 3233, 3277 [4.68572, 1.94347, 1.54572]	0
CHF$_2$OCHF$_2$ (SC2)	55, 106, 186, 374, 483, 545, 601, 638, 795, 1128, 1146, 1201, 1222, 1264, 1280, 1412, 1443, 1450, 1491, 3226, 3228 [5.32430, 1.59785, 1.49942]	0
TS1$_{SC1}$	1759i, 36, 93, 125, 155, 172, 209, 402, 404, 490, 549, 601, 711, 805, 856, 1083, 1163, 1183, 1214, 1253, 1272, 1323, 1411, 1452, 1470, 3276, 3906 [2.46249, 1.55277, 1.37522]	0.7611 (0.7840)
TS2$_{SC1}$	1807i, 17, 51, 78, 90, 134, 204, 408, 418, 472, 549, 599, 660, 792, 895, 1080, 1138, 1203, 1217, 3226, 3897 [2.88583,1.13394,1.11339]	0.7610 (0.7857)
TS$_{SC2}$	1663i, 13, 108, 119, 128, 185, 204, 373, 439, 512, 550, 582, 662, 800, 862, 1133, 1162, 1202, 1218, 1253, 1263, 1354, 1423, 1456, 1503, 3235, 3894 [2.53647, 1.42451, 1.10338]	0.7609 (0.7824)
CHF$_2$OCF$_2$ (RC1)	45, 92, 194, 402, 470, 542, 596, 661, 819, 1045, 1191, 1199, 1253, 1294, 1345, 1418, 1466, 3269 [4,79983, 1.97912, 1.57587]	0.7520 (0.7542)
CHF$_2$OCF$_2$ (RC2)	34, 76, 184, 375, 508, 550, 564, 645, 784, 1095, 1183, 1215, 1247, 1299, 1378, 1437, 1462, 3228 [5.40478, 1.53592, 1.52010]	0.7522 (0.7840)
OH	3869 [569.590503]	0.7528 (0.7547)
H$_2$O	1637, 3972, 4098 [861.61211, 431.50132, 287.51288]	0

[a] The values within parenthesis correspond to the $<S^2>$ values at the HF/6-311G** level

Rate constant calculations

The rate constant for each reaction channel of reaction (R1) is estimated, as described before, in the temperature range of 250 -1000 K using the TST expression (Eq. 1) and Eckart's unsymmetric barrier method for tunneling correction taking into account the existence of pre- and post-reaction complexes (as discussed while deriving Eq. 5). As mentioned before and shown in Fig. 2, reaction between the SC1 conformer of CHF$_2$OCHF$_2$ and OH radicals goes through two different channels RP1$_{SC1}$ and RP2$_{SC1}$ passing through TS1$_{SC1}$ and TS2$_{SC2}$, respectively. Therefore the rate constant for SC1 conformer is estimated as the sum of the rate constants for these two channels (k1$_{SC1}$ and k2$_{SC1}$). On the other hand, reaction between the SC2 conformer of CHF$_2$OCHF$_2$ and OH radicals (RP3$_{SC2}$) has only one reaction channel. The σ_r value in Eq. 1 is taken as 2 for this reaction channel due to the presence of two equivalent H-atoms. The rate constant values calculated from the G2(MP2) barrier heights for reaction channels RP1$_{SC1}$ and RP2$_{SC1}$ (k$_{SC1}$=k1$_{SC1}$+k2$_{SC1}$) and RP3$_{SC2}$ (k$_{SC2}$) are listed in Table 4.

The total rate constant (k$_{OH}$) at any temperature T is then estimated from the weighted average of the rate constant values for k$_{SC1}$ and k$_{SC2}$ as:

$$k(T) = w_{SC1}(T)[k1_{SC1}(T) + k2_{SC1}(T)] + w_{SC2}(T).k_{SC2}(T) \tag{6}$$

The w$_{SC1}$ and w$_{SC2}$ are the temperature dependent weight factors estimated from the Boltzmann population distribution law [48]. The w$_{SC1}$ is calculated as $(1/(1+exp(-\Delta E/RT))$, where ΔE is the energy difference between the SC1 and SC2 conformer; and w$_{SC2}$=1 − w$_{SC1}$. The calculated total rate constant (k$_{OH}$) values for hydrogen abstraction reactions of CHF$_2$OCHF$_2$ and OH radical within a range of 250 − 1000 K are presented in Table 4. The rate constant values for the SC1

Table 3 Relative energies (ΔE_{rel} in kcal mol^{-1} including ZPE) for all species involved in reaction channels (RP1$_{SC1}$, RP2$_{SC1}$ and RP3$_{SC2}$) of CHF$_2$OCHF$_2$ reactions with OH radical. Reaction enthalpy ($\Delta_r H_{298}^0$) and bond dissociation enthalpy (D$_{298}^0$) at 298 K as obtained at the G2 (MP2) and MPWB1K level. Data are in kcal mol^{-1}

	G2(MP2)	MPWB1K
ΔE_{rel}		
CHF$_2$OCHF$_2$ (SC1)	0	0
CHF$_2$OCHF$_2$ (SC2)	0.87	1.12
CR$_1$	−1.67	−2.50
CR$_2$	−0.73	−0.63
CR$_3$	0.56	0.27
TS1$_{SC1}$	5.33	5.27
TS2$_{SC1}$	6.08	5.96
TS$_{SC2}$	5.19	5.16
CP1	−13.91	−11.45
CP2	−16.11	−14.21
$\Delta_r H_{298}^0$		
R1$_{SC1}$	−13.01	−10.91
R1$_{SC2}$	−13.83	−11.57
Average[a]	−13.16 (-13.1)[b]	−11.03
D$_{298}^0$		
H$_2$O→HO+H	119.2 (119.0)[c]	112.5

[a] Weighted average according to the population of SC1 and SC2 conformers
[b] Calculated from reported heats of formation values. [c] Experimental value from ref [47]

Table 4 Rate constant values (cm^3 molecule^{-1} s^{-1}) for hydrogen abstraction reactions of SC1 ($k_{SC1}=k1_{SC1}+k2_{SC1}$) and SC2 ($k_{SC2}$) conformers of CHF$_2$OCHF$_2$ with OH radical and total rate constant values (k_{OH}) for reaction (R1) using G2(MP2) barrier height

T (K)	$k_{SC1}\times10^{15}$	$k_{SC2}\times10^{14}$	$k_{OH}\times10^{14}$
250	0.385	0.715	0.138
298	**0.645**	**1.27**	**0.289**
350	1.24	2.30	0.607
450	4.29	6.30	2.03
550	12.4	14.5	5.36
650	30.1	29.2	11.8
750	63.6	53.0	23.0
850	120.0	88.8	40.7
950	209.0	140.0	66.8
1000	269.0	172.0	83.6

and SC2 conformers and the total rate constant (k_{OH}) value are also shown in Fig. 3 along with the experimental results. For the reaction of CHF$_2$OCHF$_2$ with OH radical, the calculated k_{OH} value from the G2(MP2) barrier heights amounts to 2.9×10^{-15} cm^3 molecule^{-1} s^{-1} at 298 K, which agrees well with the reported experimental value of 2.4×10^{-15} cm^3 molecule^{-1} s^{-1} [27, 28]. The k_{OH} value obtained from the MPWB1K results at 298 K is 3.7×10^{-15} cm^3 molecule^{-1} s^{-1}. Figure 3 shows that the agreement between our calculated value and the available experimental results is quite good in the entire temperature range of experimental study. The rate constant (k_{Cl}) value for the CHF$_2$OCHF$_2$+Cl reaction has recently been estimated as 5.9×10^{-16} cm^3 molecule^{-1} s^{-1} at 298 K [30] which is almost five times lower than our calculated k_{OH} value. In fact, rate constant for the reaction of HFEs with OH is generally higher than the reaction between HFE and Cl atom [14].

The Arrhenius equation obtained from the calculated k_{OH} value in the temperature range of 275-410 K is: $k(T)=5.3\times$
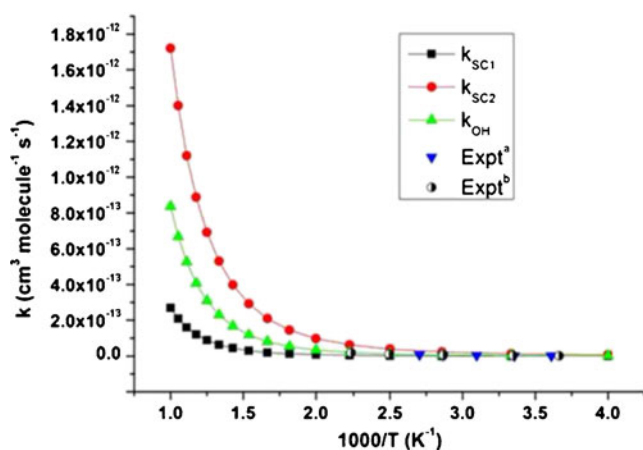

Fig. 3 Rate constants for hydrogen abstraction reactions of two conformers (SC1 and SC2) of CHF$_2$OCHF$_2$ with OH radical and total rate constant (k_{OH}) for the CHF$_2$OCHF$_2$+OH reaction [a]Ref [25] (JPCA 1999, 103, 9770); [b]Ref [27] (JPCA 2001, 105, 1445)

10^{-13} exp (-1559/T) cm^3 molecule^{-1} s^{-1} and is found to be in good agreement with that reported by Orkin et al. (0.82×10^{-12} exp(-1730±110)/T) [25] and Garland et al. ($5.4\pm3.5)\times10^{-13}$ exp(-1560±200)/T) [24]. The activation energy, E_a, value obtained from our equation (3.1 kcal mol^{-1}) is also close to the experimental value reported by Garland et al. (3.1 kcal mol^{-1}) [24] and Hsu et al. (4.0 kcal mol^{-1}) [26].

We must note that the Arrhenius plot of the total rate constant k exhibits significant non-linear behavior, mainly due to significant tunneling contribution at lower temperature range and because of contribution from different reaction channels, which makes pre-exponential factor highly temperature dependent. It is therefore better to fit the rate constant in a model equation. As a general practice, hydrogen abstraction rate constant is generally expressed by a three parameter model equation:

$$k(T) = A\,T^n\,\exp\left(-\Delta E^0/RT\right), \qquad (7)$$

where A, n and ΔE^0 are the adjustable parameters. The ΔE^0 can be taken as a hypothetical reaction barrier at 0 K and is related to the activation energy as,

$$E_a = \Delta E^0 + nRT. \qquad (8)$$

However, this three parameter model Eq. (7) could not be used for CHF$_2$OCHF$_2$+OH system because of high limit of errors in the fitting parameters. Therefore, hydrogen abstraction rate constant for this reaction is expressed by another three parameter model equation [49]:

$$k = C\,\exp\left[-\left(D_1 - \frac{D_2}{T}\right)/RT\right], \qquad (9)$$

where C, D_1 and D_2 are fitting parameters ($D_1>0$ and $D_2>0$), and R is the gas constant. Then, the corresponding activation energy, E_a, is given by:

$$E_a = D_1 - \frac{2D_2}{T}. \qquad (10)$$

The calculated rate constant for the reaction of CHF$_2$OCHF$_2$ with OH radical in the temperature range of 250-1000 K is fitted in model Eq. 9 and found to be best described by the following equation:

$$k_{OH} = 4.42 \times 10^{-11}\exp\{-(4574.5 - 500436/T)/T\}. \qquad (11)$$

The activation energy, E_a, value calculated from Eq. 8 is 2.42 kcal mol^{-1} at 298 K.

The tropospheric lifetime (τ_{eff}) of CHF$_2$OCHF$_2$ can be estimated by assuming that its removal from the atmosphere occurs only through reaction with OH radicals. Then the τ_{eff} can generally be expressed as [12],

$$\tau_{eff} \approx \tau_{OH},$$

where $\tau_{OH} = (k_{OH} \times [OH])^{-1}$ and [OH] is the global average OH radical concentration in atmosphere. Using the 298 K value of $k_{OH} = 2.9 \times 10^{-15}$ cm^3 molecule^{-1} s^{-1} and the global average atmospheric OH radical concentration of 8.8×10^5 molecules/cm^3 [50], the atmospheric lifetime for CHF_2OCHF_2 is estimated to be around 12 years. Our estimated atmospheric lifetime value is lower by about 3 years from the experimentally predicted value because the calculated k_{OH} value is slightly higher than that predicted from experiment.

Conclusions

Theoretical investigations have been carried out for the hydrogen abstraction reactions of CHF_2OCHF_2 with OH radical using ab initio G2(MP2) and DFT based MPWB1K method. This is the first detailed theoretical kinetic study of this important reaction in a wide temperature range of 250-1000 K. *The CHF_2OCHF_2 molecule has two relatively close in energy conformers (SC1 and SC2). The reaction is found to follow an indirect path through the formation of pre- and post-reactive complexes. Three important reaction channels have been identified for the reaction: two channels originating from the SC1 conformer of CHF_2OCHF_2 and the third channel from the SC2 conformer.* Our calculated total rate constant value $k_{OH} = 2.9 \times 10^{-15}$ cm^3 molecule^{-1} s^{-1} at 298 K at the G2(MP2) level is found to be in good agreement with the reported experimental results. Moreover, our results are seen to agree well with the experimental results in the entire temperature range of 250-400 K. The rate constant value obtained from the MPWB1K method (3.1×10^{-15} cm^3 molecule^{-1} s^{-1}) is found to be slightly higher than the G2(MP2) and available experimental results. We report the rate constant values for $CHF_2OCHF_2 + OH$ reactions for the first time in a wide temperature range of 250 – 1000 K. To this end, *a three parameter model equation $k_{OH} = 4.42 \times 10^{-11} \exp\{-(4574.5 - 500436/T)/T\}$ has been proposed to describe the rate constants in this temperature range. The $\Delta_r H^0_{298}$ values for $CHF_2OCHF_2 + OH$ reaction is calculated to be -13.2 kcal mol^{-1}.* Atmospheric lifetime of CHF_2OCHF_2 is estimated to be around 12 years.

References

1. Farman JD, Gardiner BG, Shanklin JD (1985) Nature 315:207–210
2. World Meteorological Organization (WMO) (1995) Scientific assessment of ozone depletion, 1994. Report no. 37. WMO, Geneva
3. Sekiya A, Misaki S (1996) ChemTech 26:44–48
4. Wallington TJ, Guschin A, Stein JNN, Platz J, Sehested J, Christensen LK, Nielsen OJ (1998) J Phys Chem A 102:1152–1161
5. Sekiya A, Misaki S (2000) J Fluorine Chem 101:215–221
6. Tsai WT (2005) J Hazardous Mater 119:69–78
7. Tokuhashi K, Takahashi A, Kaise M, Kondo S, Sekiya A, Yamashita S, Ito H (2000) J Phys Chem A 104:1165–1170
8. Dalmasso PR, Neito JD, Taccone RA, Teruel MA, Lane SI (2006) J Phys Org Chem 19:771–775
9. Kambanis KG, Lazarou YG, Papagiannakopoulos P (1998) J Phys Chem A 102:8620–8625
10. Imasu R, Suga A, Matsuno T (1995) J Meteorol Soc Jpn 73:1123–1136
11. Houghton JT et al (2001) Climate Change 2001: The scientific basis, contribution of working group I to the Third Assessment Report of the Intergovernmental Panel on Climate Change. Intergovernmental Panel on Climate Change (IPCC), Geneva
12. Papadimitriou VC, Kambanis KG, Lazarou YG, Papagiannakopoulos P (2004) J Phys Chem A 108:2666–2674
13. Oyaro N, Sellevag SR, Nielsen C (2005) J Phys Chem A 109:337–346
14. Wu JY, Liu JY, Li ZS, Sun CC (2004) Chem Phys Chem 5:1336–1344
15. Yang L, Liu JY, Wang L, He HQ, Wang Y, Li ZS (2008) J Comput Chem 29:550–561
16. Blowers P, Tetrault KF, Trujillo-Morehead Y (2008) Theor Chem Account 119:369–381
17. Jia X, Liu Y, Sun J, Sun H, Su Z, Pan X, Wang R (2010) J Phys Chem A 114:417–424
18. Chen L, Kutsuna S, Tokuhashi K, Sekiya A, Tamai R, Hibino Y (2005) J Phys Chem A 109:4766–4771
19. Zavala-Oseguera C, Alvarez-Idabo JR, Merino G, Galano A (2009) J Phys Chem A 113:13913–13920
20. Wallington TJ, Hurley MD, Nielsen OJ, Andersen MPS (2004) J Phys Chem A 108:11333–11338
21. El-Nahas AM, Uchimaru T, Sugie M, Tokuhashi K, Sekiya A (2005) J Mol Struct (THEOCHEM) 722:9–19
22. Wu JY, Liu JY, Li ZS, Sun CC (2003) J Chem Phys 118:10986–10995
23. Zhang Z, Saini RD, Kurylo MJ, Huie RE (1992) J Phys Chem 96:9301–9304
24. Garland NL, Medhurst LJ, Nelson HH (1993) J Geophys Res 98:23107–23111
25. Orkin VL, Villenave E, Huie RE, Kurylo MJ (1999) J Phys Chem A 103:9770–9779
26. Hsu KJ, DeMore WB (1995) J Phys Chem 99:11141–11146
27. Wilson EW Jr, Sawyer AA, Sawyer HA (2001) J Phys Chem A 105:1445–1448
28. Sander SP, Friedl RR, Golden DM, Kurylo MJ, Kellar-Rudek H, Wine PH, Huie RE, Orkin VL, Moortgat GK, Ravishankara AR, Kolb CE, Molina MJ, Finlayson-Pitts BJ (2006) Chemical kinetics and photochemical data for use in atmospheric studies: evaluation number 15. JPL, Pasadena
29. Good DA, Kamboures M, Santiano R, Francisco JS (1999) J Phys Chem A 103:9230–9240
30. Devi KJ, Chandra AK (2012) Curr Sci 102:470–477
31. Zhao Y, Truhlar DG (2004) J Phys Chem A 108:6908–6918
32. Zhao Y, Schultz NE, Truhlar DG (2006) J Chem Theor Comput 2:364–382
33. Devi KJ, Chandra AK (2009) Chem Phys Lett 480:161–167
34. Devi KJ, Chandra AK (2011) Comput Theor Chem 965:268–274
35. Curtiss LA, Raghavachari K, Pople JA (1993) J Chem Phys 98:1293–1298
36. Devi KJ, Chandra AK (2011) Chem Phys Lett 502:23–28

37. Frisch MJ et al. (2004) Gaussian 03, Revision C.01. Gaussian Inc, Wallingford
38. Laidler KJ (2004) Chemical Kinetics, 3rd edn. Pearson Education, New Delhi
39. Johnston HS, Heicklen J (1962) J Phys Chem 66:532–533
40. Tunneling factor $\Gamma(T)$ was estimated using our own program. Numerical integration was carried out using trapezoidal method with a stepsize of 2.5×10^{-5} and using 8×10^{6} steps
41. Chase MW Jr, Davies CA, Downey JR Jr, Frurip DJ, McDonald RA, Syverud AN (1985) JANAF thermochemical tables, 3rd edn. J Phys Chem Ref Data 14:1–926
42. Truhlar DG (1991) J Comput Chem 12:266–270
43. Singleton DL, Cvetanovic RJ (1976) J Am Chem Soc 98:6812–6819
44. Uc VH, Garcia-Cruz I, Hernandez-Laguna A, Vivier-Bunge A (2000) J Phys Chem A 104:7847–7855
45. Hammond GS (1955) J Am Chem Soc 77:334–338
46. Good DA, Francisco JS (1998) J Phys Chem A 102:7143–7148
47. Lide DR (ed) (2008-2009) CRC handbook of chemistry and physics, 89th ed. CRC, New York
48. McQuarrie DA (2003) Statistical mechanics. VIVA, New Delhi
49. Zheng J, Truhlar DG (2010) Phys Chem Chem Phys 12:7782–7793
50. Kurylo MJ, Orkin VL (2003) Chem Rev 103:5049–5076